J. Shanghai Jiao Tong Univ. (Sci.), 2023, 28(3): 323-329
https://doi.org/10.1007/s12204-023-2581-3

Visual Positioning of Nasal Swab Robot Based on Hierarchical Decision

LI Guozhi[a] (李国志), *ZOU Shuizhong*[b*] (邹水中), *DING Shuxue*[a] (丁数学)
(a. School of Artificial Intelligence; b. School of Electronic Engineering and Automation, Guilin University of Electronic Technology, Guilin 541004, Guangxi, China)

Abstract: This study focuses on a robot vision localization method for coping with the operational task of automatic nasal swab sampling. The application is important in the detection and epidemic prevention of Corona Virus Disease 2019 (COVID-19) to alleviate the large-scale negative impact of individuals suffering from pneumonia owing to COVID-19. In this method, the idea of a hierarchical decision network is used to consider the strong infectious characteristics of the COVID-19, which is followed by processing the robot behavior constraint condition. The visual navigation and positioning method using a single-arm robot for sampling is also planned, which considers the operation characteristics of medical staff. In the decision network, the risk factor for potential contact infection caused by swab sampling operations is established to avoid the spread among personnel. A robot visual servo control with artificial intelligence characteristics is developed to achieve a stable and safe nasal swab sampling operation. Experiments demonstrate that the proposed method can achieve good vision positioning for the robots and provide technical support for managing new major public health situations.
Key words: surgical robot, nasal swab sampling, vision servo, hierarchical decision
CLC number: TP 242, R 314 **Document code:** A

0 Introduction

Corona Virus Disease 2019 (COVID-19) not only presents a high infectivity but also a high concealment, which causes human respiratory symptoms or the development of pneumonia. Moreover, COVID-19 is constantly mutating, and the variants also have a certain infectivity for individuals who have been vaccinated. Therefore, the COVID-19 pneumonia significantly threatens the health of individuals and interferes with the nominal living conditions for most at a global scale[1-3]. Simultaneously, effective detection and prevention of this pandemic has become an important research topic. For the existing prevention and treatment of the COVID-19 pneumonia, the use of nasal or throat swabs to obtain nucleic acid detection samples of the tested population is the main method for diagnosis[4-6]. However, because the COVID-19 is mainly transmitted through respiratory foam and close contact, medical personnel will inevitably contact patients during the process of collecting nucleic acid test samples for medical diagnosis and treatment. There is a potential risk of viral infection among medical workers, which may cause disease transmission. Therefore, relevant scientific research institutions have attempted to use robot technology for the prevention, detection, diagnosis, and medical care of this infectious disease[7-8].

Because numerous repeated nucleic acid detection tests are often required for prevention, which is critical for controlling the COVID-19 pneumonia, a significant and boring workload is assigned to the relevant medical staff and recording errors may occur due to personnel fatigue. Therefore, the University of Southern Denmark has developed the first robotic system in the world for the detection of the COVID-19. The device uses 3D printing technology to manufacture swabs for obtaining test samples, in addition to using modular devices and open-source programmable functions. This system can achieve convenient, efficient, and low-cost automated nucleic acid screening with throat swab samples. Shanghai Jiao Tong University designed a liquid sample processing system integrated with robot modules, which can accurately detect several biological samples and effectively reduce the labor intensity of personnel to improve the efficiency of task completion while reducing the physical loss. The first generation of the semi-automatic throat swab acquisition

Received: 2022-08-27 **Accepted:** 2022-09-28
Foundation item: the Director Foundation of Guangxi Key Laboratory of Automatic Detection Technology and Instrument (No. YQ21110)
∗**E-mail:** zoushuizhong@guet.edu.cn

robot was developed by Shenyang Institute of Automation, Chinese Academy of Sciences, and the First Affiliated Hospital of Guangzhou Medical University, for which preliminary biological sample collection experiments were conducted. The system integrates a type of snake-like manipulator, equipped with binocular endoscopes that can display high-definition 3D visual scenes and can perform real-time remote interactive operations with human-computer communication through a wireless transmission function. It can conduct safe sampling tasks rapidly and effectively by sensing the contact force between the equipment and pharyngeal tissue, which improves the quality of the throat swab samples and avoids possible errors in the test results[9]. The research team from Tsinghua University has developed a navigation and positioning device for the automatic swab test system, where a Cartesian robot was used for the testing of nucleic acid samples, and a mechanical arm with 6 degrees of freedom (DOFs) with a holder can load and unload the pharyngeal swabs. The system also has the ability to perceive touch, obtains depth information, and achieves multi-modal data processing, which enables the safe collection of nucleic acid test samples to be completed[10].

Nasal swab sampling is also a common method for the prevention and control of COVID-19, which is similar to that used for pharyngeal swabs[11-13]. Both of them require obtaining mucus samples from human respiratory channels. However, the difference is that the locations of the samples are different. Compared with the throat position of throat swab sampling, the nose position is occasionally more appropriate for nucleic acid detection samples. For example, researchers have designed a small rope-tendon-driven snake-shaped soft robot arm that can be used for nasal surgery. The length and curvature of the bending part of the soft robot are controlled using rope tendon drive. This method expands the working space of the robot and enhances the dexterity of movement. Furthermore, it also has an adjustable structural stiffness, which is conducive to performing operational tasks in the narrow nasal cavity for the test[14]. Other researchers have developed a similar nasal swab collection robot with a remote operation function. The system included two master control devices and a slave device. One master control device was used to control the telescopic movement of the swab, and the other was used to control the movement state of the end-effector of the slave hand and adjust the spatial attitude of the swab. The 6-DOF parallel mechanism at the end of the hand device can move freely within a limited space range and effectively achieves non-contact swab sampling of respiratory diseases. This function is available based on combining the force sensor and visual perception[15].

Owing to the new situation in which COVID-19 virus is changing globally, researchers in various countries not only update the detection equipment, but also improve the epidemic prevention and nucleic acid sample analysis by using the artificial intelligence theory[16-18]. For example, researchers from Jilin University have used medical imaging technology to obtain high-dimensional image information that is not easily perceived visually from computed tomography (CT), and used in-depth learning method to train the data of pulmonary ground glass lesions caused by the novel coronavirus pneumonia. The results can then combine clinical features to achieve an auxiliary diagnosis with artificial intelligence characteristics[19]. Northeastern University proposed a robust segmentation mask region convolutional neural network (R-CNN) algorithm for a pharyngeal swab automatic sampling robot system, which can obtain sufficient available data based on the original image dataset. The oral images were combined with the augmentation method, which can perform reasonable image segmentation and extract accurate sample acquisition and positioning areas. The results can provide reliable guidance for robots to test nucleic acid pharyngeal swabs[20].

On the other hand, the use of robot technology can achieve numerous high-speed nucleic acid detection tasks, which is conducive to alleviating the fatigue of medical personnel during work and is also convenient for the accurate recording of test results. Currently, relevant scientific research institutions have globally evaluated the application of robots in the actual epidemic prevention process and proved that the corresponding technical scheme can obtain certain beneficial results, which is feasible and effective, and has the potential for continuous improvement. Therefore, the use of robot technology combined with the machine learning theory for nucleic acid detection sample collection can effectively reduce the risk of COVID-19 transmission in hospitals, which can effectively protect the health and safety of all individuals and help improve the detection efficiency. The prevention and control of COVID-19 and other similar infectious diseases is critical.

To solve the problem of determining the mouth position of the detected person when using the throat swab sampling robot, Shenyang University of Technology used an improved convolutional neural network model for image processing, which was combined with the multi-scale feature fusion method to improve the segmentation performance of the learning network. This method can effectively obtain valuable feature data and provide accurate positioning information for the throat swab sampling robot[21].

This study primarily focuses on the problem of visual localization of a nasal swab sampling robot.

1 Kinematics and Hierarchical Decision

Herein, the geometric background of the product of exponential (POE) formula is presented and relevant properties are introduced. Different types of robots have various mechanical structures. The kinematic models used to represent robots have different methods for formulating them, for example, the Denavit-Hartenberg (DH), POE, and complete and parametrically continuous (CPC) modeling technique[22-23]. Every model has different advantages during kinematic analysis. For example, the DH model is easy to understand and is widely used, the POE formula is singularity-free, and the CPC model is a modification of the standard parametrically continuous DH model. The most widely used method is the DH model, which formulates the kinematic equations of robots based on a homogeneous matrix transformation (HMT)[24]. Certain modifications to the standard DH convention can avoid discontinuous situations when consecutive joint axes are parallel or near parallel, for example, the CPC modeling technique[25-26]. Studies have investigated other systematic methods in order to construct kinematic models. The Lie algebra and group theory can be used to represent the pose of the end-effector despite the geometrical meaning being obscured. The POE formula can avoid the singularity problem during the pose control of the robot. This advantage has attracted the attention of several researchers investigating calibration procedures by employing the POE formula. Park and Okamura[22] first developed a formulation in order to relate kinematic errors to end-effector errors for serial chain manipulator calibrations.

It is necessary to make the basic assumption that the links of the serial robot are rigid, and the formulation of the robotic kinematic equations contains only geometrical parameters. This indicates that the functions used to calculate the pose of the end effector are based on the joint parameters and kinematic structure of the manipulator.

The POE formula describes the forward kinematic equations of a serial robot by using two frames. The first frame is the base frame {S}, x_i, y_i, z_i are the corresponding axes, and θ_i is the corresponding rotation angle. The second frame is the tool frame {T}, $x_{i\mathrm{a}}$, $y_{i\mathrm{a}}$, $z_{i\mathrm{a}}$ are the corresponding axes, and $\theta_{i\mathrm{a}}$ is the rotation angle. In addition, $\hat{q}_i$ is the dual quaternion representation of {S}; $\hat{q}_{\mathrm{f}}$ is the dual quaternion representation of {T}. This study mainly considered a serial robot. The base frame {S} was attached to the position of the basement of the surgical robot, and the tool frame {T} was attached to the end-effector of the surgical robot. Figure 1 shows a schematic of the joint frames: i represents the joint i, and "a" represents the actual pose of the joint i.

Subsequently, the forward kinematic equations of an

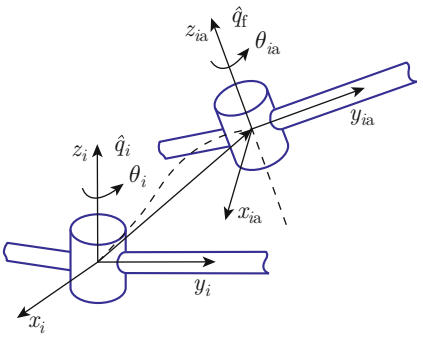

Fig. 1 Schematic of joint frames

n-DOF serial robot are given as follows:

$$g = \prod_{i=1}^{n} \exp(\hat{\boldsymbol{\xi}}_i q_i) \exp(\hat{\boldsymbol{\xi}}_{\mathrm{st}} q_{\mathrm{st}}), \tag{1}$$

$$\hat{\boldsymbol{\xi}}_i = \begin{bmatrix} \hat{\boldsymbol{\omega}}_i & \hat{\boldsymbol{\nu}}_i \\ 0 & 0 \end{bmatrix}, \tag{2}$$

where, $\boldsymbol{\nu}_i = [\nu_{1i} \quad \nu_{2i} \quad \nu_{3i}]^{\mathrm{T}} \in \mathbb{R}^3, \hat{\boldsymbol{\nu}}_i$ is the column matrix form of $\boldsymbol{\nu}_i$, $\boldsymbol{\omega}_i = [\omega_{1i} \quad \omega_{2i} \quad \omega_{3i}]^{\mathrm{T}} \in \mathbb{R}^3$, $\hat{\boldsymbol{\omega}}_i$ is the skew-symmetric matrix, and $\hat{\boldsymbol{\omega}}_i \in \mathrm{so}(3)$; q_i means the angle of the joint i, and $\exp(\hat{\boldsymbol{\xi}}_{\mathrm{st}} q_{\mathrm{st}})$ is the initial transformation from the tool frame to the base frame.

Considering completing the kinematics of the robot system, not only does it conduct the motion control operation of the robot but also performs the visual servo control. This hierarchical decision can expand the adaptability of a robot while performing different task operations. A robot system with a visual function may acquire dynamic images during the process of target positioning. It can quickly process image data and obtain the target feature information when the camera has an appropriate frame rate. Then, it can form control instructions according to the structural characteristics of the robot to realize target positioning in a three-dimensional space. The speed of the vision system while acquiring image information and processing the algorithm affects the performance of the robot. The position information of the human nostrils can be modified by stable control decisions and algorithms. The target area is then acquired using this appropriate method. Furthermore, according to the requirements of the robot system to realize target positioning, the control target of the robot visual servo system can be studied by combining it with the hierarchical decision method, as shown in Fig. 2.

The status variable set of the person's face target is $\boldsymbol{X}_t^{\mathrm{p}}$, including the spatial location of the target $\boldsymbol{y}_t$, speed $\boldsymbol{v}_t$, damping coefficient $\boldsymbol{d}_t$ and other interference coefficients $\boldsymbol{k}_t$. Herein, t is time slice and

$$\boldsymbol{X}_t^{\mathrm{p}} = [\boldsymbol{y}_t^{\mathrm{T}} \quad \boldsymbol{v}_t^{\mathrm{T}} \quad \boldsymbol{d}_t^{\mathrm{T}} \quad \boldsymbol{k}_t^{\mathrm{T}}]^{\mathrm{T}}. \tag{3}$$

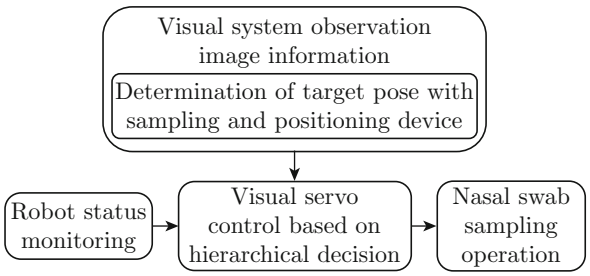

Fig. 2 Schematic of hierarchical decision

Generally, it can be considered that the current state of the target at the time t in the physical space does not depend too much on the actual state of the target before the time t. However, to locate the target, the hand-eye system needs to be able to predict the target. Using the characteristics of the target with Markov attributes, the target state in a finite time slice can be selected to infer the target characteristics of the future time slice $t+1$, that is to obtain the state variable set $\boldsymbol{X}_{t+1}^{\mathrm{p}}$. The robot vision localization method is included in the hierarchical decision of the robot control system. The static positioning information of the nostrils when the robot samples nasal swabs is the main consideration for safety. The robot will stop if there is an instinctive reaction of shaking the head slightly during nasal swab sampling of one person. However, the robot can restart the procedure if the vision system captures the action of the person in a predetermined range of view.

When the observation target entered the field of view, Gaussian estimation was performed based on the range of the region in the image coordinate system, and the observation error was introduced into the observation equation.

Dynamic Bayesian network is combined to analyze and predict the motion state of the target:

$$P(\boldsymbol{x}_{t+1}^{\mathrm{p}}|\boldsymbol{x}_t^{\mathrm{p}}) = N(\mu_{\boldsymbol{x}}, \sigma_{\boldsymbol{x}}^2), \tag{4}$$

$$P(\boldsymbol{y}_{t+1}|\boldsymbol{x}_t^{\mathrm{p}}, \boldsymbol{y}_t) = N(\mu_{\boldsymbol{y}}, \sigma_{\boldsymbol{y}}^2)N(\mu_{\boldsymbol{x}}, \sigma_{\boldsymbol{x}}^2), \tag{5}$$

where, $\boldsymbol{x}_t^{\mathrm{p}}$ is the status variable of each component; $P(\boldsymbol{x}_{t+1}^{\mathrm{p}}|\boldsymbol{x}_t^{\mathrm{p}})$ is the transfer model of the status variable $\boldsymbol{X}_t^{\mathrm{p}}$; $P(\boldsymbol{y}_{t+1}|\boldsymbol{x}_t^{\mathrm{p}}, \boldsymbol{y}_t)$ is the conditional probability transition model of the status variable $\boldsymbol{X}_t^{\mathrm{p}}$ and observable evidence variable $\boldsymbol{y}_t$; $N(\mu_{\boldsymbol{x}}, \sigma_{\boldsymbol{x}}^2)$ and $N(\mu_{\boldsymbol{y}}, \sigma_{\boldsymbol{y}}^2)$ are the corresponding normal distribution functions.

With a continuous time slice, the dynamic network is spread out to observe the complete tracking sequence of the robot system. The vision system provides state information of the target and predicts the state of the target in the next time slice. The robot system controls the manipulator to approach the space area where the nostril region is located according to the prediction results and realizes a safe approach movement. Furthermore, the feasible motion space regions from the end effector of the robot to the target are divided into n classes. In each class, the trajectory of the manipulator is not unique. After the robot obtains the target information from the vision system, the process of controlling the manipulator to perform the approach action begins at its initial state, from the k-class space region to the specified pose.

2 System Structure of Nasal Swab Sampling Robot

According to the operation characteristics of medical personnel in the process of epidemic prevention and control, a single-arm robot was used to simulate the movement of human arms to assist in the preservation or transfer of samples into test tubes.

First, kinematic model of a single-arm robot system is established. In the actual operation of nucleic acid collection, on the one hand, it is necessary to consider the reasonable relative position and orientation difference between the robot and the detected person to avoid personal injury. However, it is also necessary to coordinate the motion state between the manipulator and the detected person to achieve accurate visual positioning and ensure the quality of sampling. At this time, the visual feedback information can be processed using artificial intelligence, and the robot can obtain an accurate positioning of the detection target. A hierarchical network can be established to safely determine the hand-eye coordination operation method.

As shown in Fig. 3, the sampling system consists of a single-arm robot and a vision system. One Franka robot was used for the study, and the system model of a single-arm robot was established as the first step.

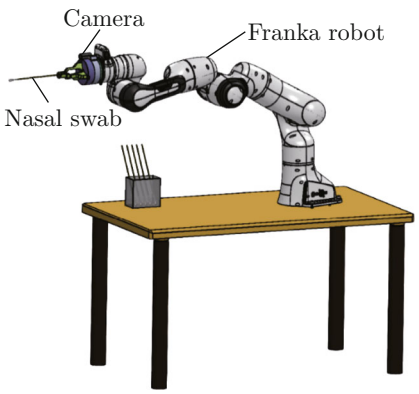

Fig. 3 Schematic diagram of nasal swab sampling robot system

The Franka robot is a flexible, sensitive, and intelligent lightweight 7-axis robot with precise force control. The camera is a CCD vision system that can be connected to the robot control laptop by the USB port, and the camera function is programmed using OpenCV. The control system can be connected to the computer, and it also opens the underlying C++ interface and a

stable secondary development platform.

Considering that the visual positioning effect of the robot system affects the control quality in the operation process, a hierarchical network is constructed and combined with the utility function to achieve the visual servo operation with a decision-making ability to improve the adaptability of the hand-eye robot system to an external changeable environment. Furthermore, the localization accuracy can be improved. On the premise of meeting the safe interaction between the robot system and the person, it can accurately determine the sampling position and perform the sampling operation.

3 Experiment and Analysis

In order to verify the effectiveness of the nasal swab sampling robot system and aforementioned hierarchical decision method, a real experiment was conducted on the serial robot. The experiment contained a single-arm redundant robot, Franka, and an RGB camera mounted at the sixth joint of the robot. The camera could observe the nasal swab clamped by the robot. The kinematics was established during the experiment, and the robot system was controlled by a computer.

Figure 4 shows the nose model used in the experiment, which was printed using a 3D printer. This model has a nominal human size and is fixed on a tripod.

Fig. 4 Nose model printed by 3D printer

Figure 5 shows the robot approaching the nostril during the procedure, and the nasal swab has not yet contacted the nose. Figure 6 shows the robot performing nasal swab sampling from the view of the camera, and the robot successfully obtained the nasal swab.

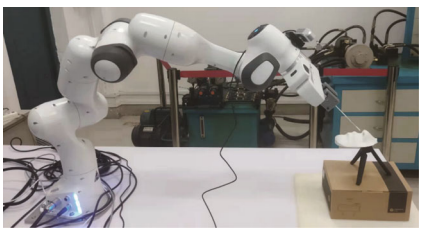

Fig. 5 Robot approaching nostril

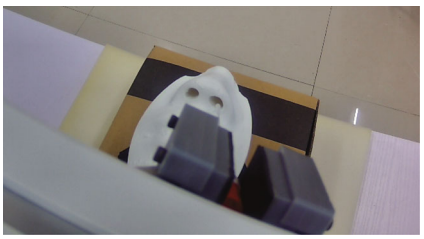

Fig. 6 Robot performing nasal swab sampling

Figure 7 shows the time consumption for processing image frames, and the distance l is between the end of the nasal swab and the center of the nose model. As the distance increased, the time consumption also increased, while the orientation remained consistent.

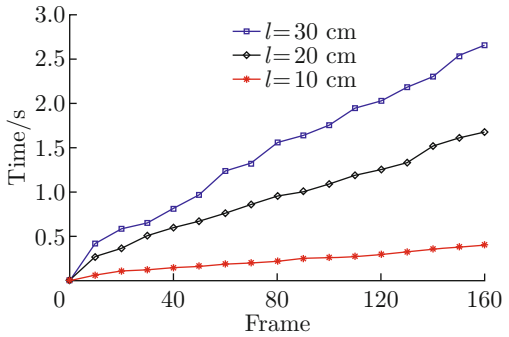

Fig. 7 Time consumption of processing image frames in total at different distances but with the same orientations

Figure 8 shows the time consumption of the test groups with different orientations but at the same distance. The time consumption is different when the orientations change, as the robot requires time for the adjustment of the end-effector to approach the nose model appropriately.

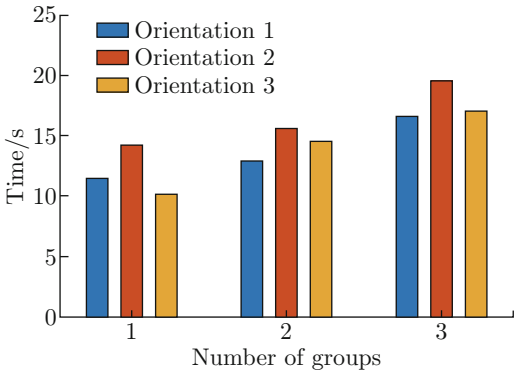

Fig. 8 Time consumption of the test groups with different orientations but at the same distance

Based on the existing experimental results, the use of robot technology can avoid direct contact between medical personnel and virus-infected or potentially infected

people and can achieve the timely detection in an isolated environment for the observed person. It can also provide doctors with remote assistance for the diagnosis and treatment of infectious diseases combined with artificial intelligence and can monitor the symptoms of patients in real time. Furthermore, the results of the experiment can provide a normal way of using robots to complete manual work, not only to perform nasal swab sampling but also any other hazardous work in a normal human environment.

4 Conclusion

A hierarchical decision method for precise nasal swab sampling is presented in this study. Forward kinematics for the serial robot was formulated. A nasal swab sampling experiment based on the proposed method was conducted on a serial robot. The POE formula was used to calculate the kinematic equations of the serial robot in a compact manner, and the corresponding control condition was efficient. A method of target location and hand-eye coordination control for a robot vision system with decision-making ability was proposed. This method can solve the problem of reliable acquisition of foreground region information, and enable the robot system to effectively process dynamic data in disturbed images. An accurate location of the sampling position was achieved and the sampling task of obtaining nucleic acid samples can be completed. This experiment validated the effectiveness of the method presented in this study.

References

[1] CHEN A T, RYSKINA K L, JUNG H Y. Long-term care, residential facilities, and COVID-19: An overview of federal and state policy responses [J]. *Journal of the American Medical Directors Association*, 2020, **21**(9): 1186-1190.

[2] FISHER D, HEYMANN D. Q&A: The novel coronavirus outbreak causing COVID-19 [J]. *BMC Medicine*, 2020, **18**(1): 57.

[3] TSIKALA VAFEA M, ATALLA E, GEORGAKAS J, et al. Emerging technologies for use in the study, diagnosis, and treatment of patients with COVID-19 [J]. *Cellular and Molecular Bioengineering*, 2020, **13**(4): 249-257.

[4] DING W P, NAYAK J, SWAPNAREKHA H, et al. Fusion of intelligent learning for COVID-19: A state-of-the-art review and analysis on real medical data [J]. *Neurocomputing*, 2021, **457**: 40-66.

[5] NAREN N, CHAMOLA V, BAITRAGUNTA S, et al. IoMT and DNN-enabled drone-assisted COVID-19 screening and detection framework for rural areas [J]. *IEEE Internet of Things Magazine*, 2021, **4**(2): 4-9.

[6] WANG X V, WANG L H. A literature survey of the robotic technologies during the COVID-19 pandemic [J]. *Journal of Manufacturing Systems*, 2021, **60**: 823-836.

[7] WU S Z, WU D D, YE R Z, et al. Pilot study of robot-assisted teleultrasound based on 5G network: A new feasible strategy for early imaging assessment during COVID-19 pandemic [J]. *IEEE Transactions on Ultrasonics, Ferroelectrics, and Frequency Control*, 2020, **67**(11): 2241-2248.

[8] XIE Z X, CHEN B H, LIU J Q, et al. A tapered soft robotic oropharyngeal swab for throat testing: A new way to collect sputa samples [J]. *IEEE Robotics & Automation Magazine*, 2021, **28**(1): 90-100.

[9] PETRUZZI G, DE VIRGILIO A, PICHI B, et al. COVID-19: Nasal and oropharyngeal swab [J]. *Head & Neck*, 2020, **42**(6): 1303-1304.

[10] MCDERMOTT A. Inner Workings: Researchers race to develop in-home testing for COVID-19, a potential game changer [J]. *Proceedings of the National Academy of Sciences of the United States of America*, 2020, **117**(42): 25956-25959.

[11] LI Z, FEILING J, REN H L, et al. A novel tele-operated flexible robot targeted for minimally invasive robotic surgery [J]. *Engineering*, 2015, **1**(1): 73-78.

[12] SEO J, SHIM S, PARK H, et al. Development of robot-assisted untact swab sampling system for upper respiratory disease [J]. *Applied Sciences*, 2020, **10**(21): 7707.

[13] SHI F, WANG J, SHI J, et al. Review of artificial intelligence techniques in imaging data acquisition, segmentation, and diagnosis for COVID-19 [J]. *IEEE Reviews in Biomedical Engineering*, 2021, **14**: 4-15.

[14] HUSSAIN K, WANG X S, OMAR Z, et al. Robotics and artificial intelligence applications in manage and control of COVID-19 pandemic [C]//*2021 International Conference on Computer, Control and Robotics*. Shanghai: IEEE, 2021: 66-69.

[15] MBUNGE E, MILLHAM R C, SIBIYA M N, et al. Framework for ethical and acceptable use of social distancing tools and smart devices during COVID-19 pandemic in Zimbabwe [J]. *Sustainable Operations and Computers*, 2021, **2**: 190-199.

[16] MEI X Y, LEE H C, DIAO K Y, et al. Artificial intelligence-enabled rapid diagnosis of patients with COVID-19 [J]. *Nature Medicine*, 2020, **26**(8): 1224-1228.

[17] XU X B, YANG Y M, ZHOU Y Y, et al. Image segmentation of throat swab sampling based on mask R-CNN [C]//*2020 Chinese Automation Congress*. Shanghai: IEEE, 2020: 7451-7455.

[18] ZHAO Z Y, WANG T, WANG D Q. Inverse kinematic analysis of the general 6R serial manipulators based on unit dual quaternion and Dixon resultant [C]//*2017 Chinese Automation Congress*. Jinan: IEEE, 2017: 2646-2650.

[19] HE R B, ZHAO Y J, YANG S N, et al. Kinematic-parameter identification for serial-robot calibration based on POE formula [J]. *IEEE Transactions on Robotics*, 2010, **26**(3): 411-423.

[20] STONE H, SANDERSON A. A prototype arm signature identification system [C]//*1987 IEEE International Conference on Robotics and Automation*. Raleigh: IEEE, 1987: 175-182.

[21] WU L, YANG X D, CHEN K, et al. A minimal POE-based model for robotic kinematic calibration with only position measurements [J]. *IEEE Transactions on Automation Science and Engineering*, 2015, **12**(2): 758-763.

[22] ASPRAGATHOS N A, DIMITROS J K. A comparative study of three methods for robot kinematics [J]. *IEEE Transactions on Systems*, *Man*, *and Cybernetics*, *Part B* (*Cybernetics*), 1998, **28**(2): 135-145.

[23] WANG W, WANG G, YUN C. A calibration method of kinematic parameters for serial industrial robots [J]. *Industrial Robot*: *An International Journal*, 2014, **41**(2): 157-165.

[24] HAGN U, KONIETSCHKE R, TOBERGTE A, et al. DLR MiroSurge: A versatile system for research in endoscopic telesurgery [J]. *International Journal of Computer Assisted Radiology and Surgery*, 2010, **5**(2): 183-193.

[25] CHEN S F, KAO I. Conservative congruence transformation for joint and Cartesian stiffness matrices of robotic hands and fingers [J]. *The International Journal of Robotics Research*, 2000, **19**(9): 835-847.

[26] WANG Y N, XU Z C, ZHAO H C, et al. M-region segmentation of pharyngeal swab image based on improved U-net model [C]//*2021 IEEE International Conference on Intelligence and Safety for Robotics*. Tokoname: IEEE, 2021: 186-190.

[27] PARK F C, OKAMURA K. Kinematic calibration and the product of exponential formula [M]// Advance in robot kinematics and computational geometry. Dordrecht: Springer, 1994: 119-128.